Radio Frequency Interference Effects of Continuous Sinewave Signals on Telemetry Data

P. W. Low
Network Operations Office

This report presents the results of an investigation of continuous sinewave interference effects on telemetry data based on testing at the Goldstone Deep Space Station (DSS 11) in 1976. To analyze the effects, the continuous sinewave interference is treated as an extraneous noise. Empirical telemetry data degradation and drop-lock models are then developed based on test data and certain physical characteristics of the telemetry data processing system. These models will be used as a portion of the radio frequency interference detection tools in the first version of the Deep Space Interference Prediction software.

I. Introduction

There has been an increasing number of radio frequency interference (RFI) incidents occurring throughout the Deep Space Network (DSN) during spacecraft tracking operations in recent years. In many of these incidents the desired signal and the telemetry data processing performance were degraded, and in some severe cases the receiver and telemetry were knocked out of lock. Other than the basic observation and reporting of the RFI phenomenon, little could be done to avoid or minimize the impacts. From the DSN spacecraft tracking operations standpoint, a thorough investigation of the RFI effects was needed in order to develop a capability for:

(1) Prediction of possible RFI occurrence from a set of known sources, so that action could be taken to avoid or minimize the impacts and data loss.

(2) Prediction of possible RFI occurrence for future planning of DSN critical mission phases, and spectrum utilization of future missions.

There was very little material available either based on theoretical approach or experimental results that was applicable in analyzing the performance of the DSN spacecraft tracking and telemetry processing system in the presence of interfering signals. Therefore, an experimental approach was used. RFI tests were formulated and conducted with standard Deep Space Station (DSS) equipment to investigate continuous sinewave (CW) interference effects on the bit signal-to-noise ratio (SNR) and bit error rate (BER) of a telemetry signal. This article describes these tests and presents the empirical telemetry SNR and BER degradation and drop-lock models derived from the test data based on certain physical characteristics of the telemetry data processing system used.

II. Test Setup

A block diagram of the test configuration is shown in Fig. 1. The carrier tracking and telemetry data processing system is the standard DSS equipment. The Simulation Conversion Assembly was used to generate two binary data

streams; each data stream bi-phase-modulated a squarewave subcarrier. The two composite (data plus subcarrier) signals were then mixed and phase-modulated a continuous sinewave carrier. Operations support softwares were used in the Telemetry and Command Processor (TCP) and the Digital Instrumentation Subsystem (DIS) to provide the telemetry data BER and SNR and carrier tracking doppler phase jitter statistics respectively.

III. Pilot Study and Results

A preliminary quick-look test was performed to isolate the frequency spectrum regions where the CW interfering signal could cause "problems" to the desired signal. The results showed that:

(1) There were severe telemetry bit SNR and BER degradations when the CW interfering signal was near or on the subcarrier odd harmonics of the desired downlink signal.

(2) There was no observable degradation on telemetry data when the CW interfering signal was near or on the subcarrier even harmonics of the desired downlink signal.

(3) There were severe tracking doppler phase jitter degradation and telemetry bit SNR and BER degradations when the CW interfering signal was within 1000 Hertz of the desired downlink carrier.

(4) There was no observable degradation on tracking doppler phase jitter when the CW interfering signal was near or on any subcarrier harmonic of the desired downlink signal.

These results clearly indicated that the CW interfering signal causes two types of effect. They are:

(1) *Telemetry interference:* when the CW interfering signal is in the subcarrier or subcarrier odd harmonic spectra of the desired downlink signal.

(2) *Receiver interference:* when the CW interfering signal is within the receiver's theoretical carrier capture range ($\approx$ 1000 Hertz).

The frequency region for telemetry interference is much wider than the region for receiver interference. Thus, the probability of having telemetry interference during an RFI incident is much higher. Therefore, the characteristics of telemetry interference were first investigated by means of the following series of tests.

IV. Telemetry Interference Test

A. Test Objective

The test objective was to characterize the telemetry data bit SNR and BER degradations and the telemetry drop-lock conditions in the presence of a CW interfering signal.

B. Desired Downlink Signal Configuration

The desired downlink signal used for the test was a typical Viking spacecraft dual-subcarrier downlink signal. However, only the effects on the high rate subcarrier were investigated. Table 1 summarizes the exact desired downlink signal configuration.

C. Test Cases

Forty-two RFI cases were tested. They may be categorized into four different sets:

(1) *CW signal coincident with subcarrier:* The CW signal was placed coincident with the lower and upper subcarriers.

(2) *Subcarrier sweep:* The CW signal was swept across the subcarrier.

(3) *Subcarrier third harmonic sweep:* The CW signal was swept across the subcarrier third harmonic.

(4) *Subcarrier fifth harmonic sweep:* The CW signal was swept across the subcarrier fifth harmonic.

Tables 2 through 5 summarize the test cases performed.

V. Bit Signal-to-Noise Ratio Degradation Analysis (Non-Drop-Lock Cases)

A. Method of Approach

In analyzing the bit signal-to-noise ratio (SNR) degradation, the CW interfering signal is treated as an extraneous noise.

The presence of this CW interfering signal causes an increase in the system's noise which in turn causes an increase in the effective system noise temperature. The increased system noise temperature is then derived from the test data. Finally, a SNR degradation model is constructed based on the physical characteristics of the telemetry data processing system used.

B. SNR Degradation Model

Let Fig. 2 be the simplified system configuration used for the test. Thus, when the RFI signal is not present, the received bit SNR is:

$$SNR_I = 10 \log \left(\frac{P_D T_B}{N_S} \right)$$

where

P_D = total high rate data power

BR = bit (symbol) rate

T_B = bit (symbol) time $(1/BR)$

N_S = noise spectral density when RFI is not present

When the RFI signal is present, the received bit SNR is:

$$SNR_{IR} = 10 \log \left(\frac{P_D T_B}{N_{SR}} \right)$$

where

N_{SR} = noise spectral density when RFI is present

Then, the received bit SNR degradation is:

$$\Delta SNR_I = SNR_I - SNR_{IR}$$

or

$$\Delta SNR_I = 10 \log \left(\frac{P_D T_B}{N_S} \right) - 10 \log \left(\frac{P_D T_B}{N_{SR}} \right)$$

$$\Delta SNR_I = 10 \log \left(\frac{N_{SR}}{N_S} \right)$$

Substituting $N_S = KT_S$ and $N_{SR} = KT_{SR}$, the above equation becomes

$$\Delta SNR_I = 10 \log \left(\frac{KT_{SR}}{KT_S} \right)$$

$$\Delta SNR_I = 10 \log \left(\frac{T_{SR}}{T_S} \right)$$

where

T_S = effective system noise temperature when RFI is not present (It is also referred to as SNT)

T_{SR} = effective system noise temperature when RFI is present

K = Boltzmann's constant

Let T_R = increased system noise temperature induced by the CW interfering signal

Then,

$$T_{SR} = (T_S + T_R)$$

Therefore,

$$SNR_I = 10 \log \left(\frac{T_S + T_R}{T_S} \right) \quad (1)$$

Also, when the RFI signal is not present, the SSA bit SNR is:

$$SNR_O = SNR_I - L_S$$

When the RFI signal is present, the SSA bit SNR is:

$$SNR_{OR} = SNR_{IR} - L_{SR}$$

where L_S and L_{SR} are system losses. These include waveform distortion loss, receiver (radio) loss, subcarrier demodulator loss, and bit sync/detection loss; they are assumed to be strictly a function of the received bit SNR for a given system and configuration. Therefore, the SSA bit SNR degradation is:

$$\Delta SNR_O = SNR_O - SNR_{OR}$$

or

$$\Delta SNR_O = \Delta SNR_I - (L_S - L_{SR}) \quad (2)$$

Having Eqs. (1) and (2) established, the next step is to determine the functional relationship of the CW interfering signal and the increased system noise temperature it induces.

C. Interfering Signal Coincident with Subcarrier

The functional relationship of the CW interfering signal and the increased system noise temperature for the interfering signal coincident with the subcarrier is to be determined in this subsection. Let us examine Eq. (1) again.

$$\Delta SNR_I = 10 \log \left(\frac{T_S + T_R}{T_S} \right)$$

Solving for T_R, then:

$$T_R = T_S \left[10^{\frac{\Delta SNR_I}{10}} - 1 \right]$$

Substituting

$$\Delta SNR_I = \Delta SNR_O + (L_S - L_{SR}),$$

then:

$$T_R = T_S \left[10^{\frac{\Delta SNR_O + (L_S - L_{SR})}{10}} - 1 \right] \qquad (3)$$

From Eq. (3), T_R for each test case (1A through 1Z) is calculated. Note:

ΔSNR_O = data obtained from test cases 1A through 1Z.

L_S and L_{SR} = estimated from the Telemetry Analysis Program (TAP) by using an iterative method. See Fig. 3 for a plot of the system loss vs received bit SNR generated by the TAP for the configuration used for the test.

Then, using a trial and error method, T_R is curve fitted. The result is

$$T_R \Big|_{\Delta f_{1sc}=0, BR=2K} = \left[\left(10^{.821 e^{.0421 P_{RFI}}} \right)^2 + (40)^2 \right]^{1/2} - 39.5 \qquad (4)$$

where

Δf_{1sc} = frequency separation between the CW interfering signal and the subcarrier

P_{RFI} = RFI signal level

Using Eqs. (1) and (4), the curve fitted values are plotted against the observed values (ΔSNR_I vs P_{RFI}) as shown in Figs. 4 and 5.

D. Interfering Signal at Various Frequency Offsets from Subcarrier or Subcarrier Harmonics

The RFI effect with the CW interfering signal at various frequency offsets from the subcarrier or subcarrier harmonics will be investigated in this subsection, but let us first examine the frequency response of the telemetry system used for the test.

The telemetry system used for the test must be able to pass the antipodal binary-valued data signal in the subcarrier harmonic spectra. Therefore, it must have an impulse response:

$$h(\tau) = \begin{cases} \frac{h}{n} & 0 \leq \tau \leq T_B \\ 0 & \tau < 0, \tau > T_B \end{cases}$$

where

h = gain

n = subcarrier harmonic number, $n = 1, 3, 5$, etc.

T_B = bit time $(1/BR)$

Then, its frequency response is

$$H(n, \Delta f_{nsc}) = \int_0^\infty h(\tau) \left[e^{-j2\pi \Delta f_{nsc} \tau} \right] d\tau$$

$$= \frac{h}{n} \int_0^{T_B} \left[e^{-j2\pi \Delta f_{nsc} \tau} \right] d\tau$$

$$= \frac{h}{n} \left[\frac{e^{-j2\pi \Delta f_{nsc} \tau}}{-j2\pi \Delta f_{nsc}} \right]_0^{T_B}$$

$$= \frac{h}{n} \left[\frac{e^{-j2\pi \Delta f_{nsc} T_B} - 1}{-j2\pi \Delta f_{nsc}} \right]$$

$$= \frac{h}{n\pi\Delta f_{nsc}}$$

$$\cdot \left[\frac{e^{-j\pi\Delta f_{nsc}T_B} - e^{j\pi\Delta f_{nsc}T_B}}{-j2}\right] e^{-j\pi\Delta f_{nsc}T_B}$$

where

$$\Delta f_{nsc} = \begin{cases} |(f_c + f_{nsc}) - f_{RFI}| & \text{if } f_{RFI} > f_c \\ |(f_c - f_{nsc}) - f_{RFI}| & \text{if } f_{RFI} < f_c \end{cases}$$

where $n = 1, 3, 5$, etc.

f_{nsc} = nth harmonic of subcarrier, where $n = 1, 3, 5$, etc. $(n \cdot f_{sc1})$ (1st harmonic is also referred to as subcarrier)

f_{RFI} = RFI signal frequency

Using the Euler's identity:

$$\sin\theta = \frac{e^{j\theta} - e^{-j\theta}}{j2}$$

$$H(n, \Delta f_{nsc}) = \frac{h}{n\pi\Delta f_{nsc}} (\sin\pi\Delta f_{nsc}T_B)\left(e^{-j\pi\Delta f_{nsc}T_B}\right)$$

$$= \frac{h\,T_B}{n}\left(\frac{\sin\pi\Delta f_{nsc}T_B}{\pi\Delta f_{nsc}T_B}\right)\left(e^{-j\pi\Delta f_{nsc}T_B}\right)$$

Thus:

$$|H(n, \Delta f_{nsc})|^2 = \left[\frac{h\,T_B}{n}\left(\frac{\sin\pi\Delta f_{nsc}T_B}{\pi\Delta f_{nsc}T_B}\right)\left(e^{-j\pi\Delta f_{nsc}T_B}\right)\right]$$

$$\cdot \left[\frac{h\,T_B}{n}\left(\frac{\sin\pi\Delta f_{nsc}T_B}{\pi\Delta f_{nsc}T_B}\right)\left(e^{j\pi\Delta f_{nsc}T_B}\right)\right]$$

$$|H(n, \Delta f_{nsc})|^2 = \left(\frac{h\,T_B}{n}\right)^2 \left(\frac{\sin\pi\Delta f_{nsc}T_B}{\pi\Delta f_{nsc}T_B}\right)^2$$

For a CW signal with power (P) and one-sided power spectral density function $\{G(\Delta f_{nsc}) = (P/2)\,[\delta(\Delta f_{nsc} - \Delta f^{\star}_{nsc})]\}$ input into this telemetry system, the output power response is

$$P(n, \Delta f^{\star}_{nsc}) = \int_{-\infty}^{\infty} |H(n, \Delta f_{nsc})|^2\, G(\Delta f_{nsc})\, d(\Delta f_{nsc})$$

Using the sampling property of impulses, that is

$$\int_b^c f(\lambda)\, U_0(\lambda - a)\, d\lambda = f(\lambda) \quad \text{for } b < a < c$$

$$P(n, \Delta f^{\star}_{nsc}) = (P)\left(\frac{h\,T_B}{n}\right)^2 \left(\frac{\sin\pi\Delta f^{\star}_{nsc}T_B}{\pi\Delta f^{\star}_{nsc}T_B}\right)^2$$

Therefore, the output power response function of the telemetry system for any CW signal with power (P) is

$$P(n, \Delta f_{nsc}) = (P)\left(\frac{h\,T_B}{n}\right)^2 \left(\frac{\sin\pi\Delta f_{nsc}T_B}{\pi\Delta f_{nsc}T_B}\right)^2$$

Let

$$n = 1,$$

and

$$\Delta f_{nsc} = 0,$$

then

$$P(1,0) = (P)(h\,T_B)^2$$

Thus,

$$\left.\frac{P(n, \Delta f_{nsc})}{P(1,0)}\right|_{BR=2K} = \left(\frac{1}{n^2}\right)\left(\frac{\sin\pi\Delta f_{nsc}T_B}{\pi\Delta f_{nsc}T_B}\right)^2$$

or (expressed in decibel format)

$$P(n, \Delta f_{nsc}) = P(1,0) - 20\log n + 10\log\left(\frac{\sin\pi\Delta f_{nsc}T_B}{\pi\Delta f_{nsc}T_B}\right)^2$$

(The above result appears to be suitable for modelling SNR degradation for any bit rate. However, without test data to substantiate this claim, the scope of this model is limited to two thousand (2K) bits per second data in this analysis.)

$P(n, \Delta f_{nsc})$ is the system's power response to the CW interfering signal at any frequency offset (Δf_{nsc}), and $P(1, 0)$ is the system's power response to the CW interfering signal with Δf_{1sc} equal to zero. Also, remember that Eq. (4) obtained in the preceding subsection is based on the interfering signal level (P_{RFI}) with Δf_{1sc} equal to zero. Thus, Eq. (4) may be generalized as

$$T_R\Big|_{BR=2K} = \left[\left(10^{.821e^{.0421 P_I}}\right)^2 + (40)^2\right]^{1/2} - 39.5 \tag{5}$$

where

$$P_I = P_{RFI} - 20 \log n + 10 \log \left[\frac{\sin \Delta f_{nsc} \left(\frac{\pi}{BR}\right)}{\Delta f_{nsc} \left(\frac{\pi}{BR}\right)}\right]^2$$

n = number of the subcarrier harmonic which the interfering signal is affecting.

Using Eqs. (1) and (5), the modeled values are compared with test data. The results show that the model's bit SNR degradation predictions are slightly but consistently less than the degradation indicated by the test data. Two "adjustment factors" are then introduced into Eq. (5) to compensate for this disparity. Thus, the model becomes:

$$P_I = P_{RFI} - (0.94)(20 \log n) + (0.90) \cdot \left[10 \log \left(\frac{\sin \left(\Delta f_{nsc} \left(\frac{\pi}{BR}\right)\right)}{\Delta f_{nsc} \left(\frac{\pi}{BR}\right)}\right)^2\right] \tag{6}$$

$$T_R\Big|_{BR=2K} = \left[\left(10^{.821e^{.0421 P_I}}\right)^2 + (40)^2\right]^{1/2} - 39.5 \tag{7}$$

$$SNR_I = 10 \log \left(\frac{T_S + T_R}{T_S}\right) \tag{1}$$

$$\mathrm{SNR}_O = \Delta SNR_I - (L_S - L_{SR}) \tag{2}$$

(The observed disparity is probably caused by the "impurity" of the CW interfering signal. Because of this "impurity", the interfering signal does not have a perfect line spectrum; consequently, the resulting integral evaluation of the power response function, $P(n, \Delta f_{nsc})$, is only a close approximation. Therefore, the "adjustment factors" are needed in Eq. (6).)

The refined model (Eqs. (1), (2), (6) and (7)) predictions are compared with the test data for the eight telemetry non-drop-lock cases (2F, 3C through 3E, and 4B through 4E). The results are plotted on Figs. 6 through 13.

VI. Bit Error Rate Degradation Analysis

With no RFI, bit errors for uncoded data transmitted over a gaussian channel and detected in white additive noise are statistically independent of each other, and the BER (error probability) is

$$BER = P_E = 1/2 \; erfc \; \sqrt{\lambda}$$

where $\lambda = SNR_O$. The corresponding BER and λ values are tabulated in Table 6, and will be referred to as the "theoretical curve"

When a CW interfering signal is present, the bit errors may not be independent of each other; they may come in bursts. Consequently, the BER_R and SNR_{OR} relationship may not be the same as prescribed by the "theoretical curve." In fact, the test data show that

$$BER_R = 1/2 \; erfc \; \sqrt{\lambda}$$

where

$$\lambda = SNR_O - k(\Delta SNR_O)$$

$$k < 1$$

The coefficient k appears to be a function of SNR_O and ΔSNR_O. However, because it varies over a very small range, for practical purposes, a first-order approximation is used in this analysis. Thus, k is chosen to be 0.79 and the result is

$$BER_R = 1/2 \; erfc \; \sqrt{\lambda} \tag{8}$$

where

$$\lambda = SNR_O - 0.79 (\Delta SNR_O)$$

$$= SNR_O (0.21) + SNR_{OR} (0.79)$$

(If k were 1, then Eq. (8) would become:

$$BER_R = 1/2\ erfc\ \sqrt{SNR_O - \Delta SNR_O}$$

$$= 1/2\ erfc\ \sqrt{SNR_{OR}} = P_E$$

That is: BER_R function behaves as the "theoretical curve.")

Using Eq. (8) and Table 6, calculated BER_R values are plotted against the test data and the "Theoretical Curve" on Figs. 14 through 17 for the test cases of interfering signal coincident with the subcarrier.

The RFI-BER model (Eqs. (1), (2), (6), (7), and (8)) predictions are compared with the test data for seven frequency-sweep telemetry non-drop-lock cases as shown on Figs. 18 through 24. (For the frequency-sweep test, the BER_R test data have a resolution of only 10^{-4}. Therefore, Test case 4E, which has BER_R's considerably less than 10^{-4}, is not plotted for comparison. Also, other data points which have BER_R's less than 10^{-4} are arithmetically averaged over a longer sample (time, or Δf_{nsc}) base.)

VII. Telemetry Drop-Lock Analysis

When an interfering signal is present in a communication system, it may not only degrade the desired signal, but may also, in some severe cases, cause the communication system to drop lock. In fact, during the performance of this RFI test, eight telemetry (SDA) drop-lock cases were observed. These drop-lock cases will be discussed in this section.

Normally, it is assumed that the major cause for a telemetry system to drop lock is that the bit SNR is below threshold. However, by comparing the SNR_R predicted by the degradation model obtained in the preceding sections with test data (RFI signal level and Δf_{nsc} at which drop-lock occurs) it is found that this is not so. It is because the SNR_R predicted by the model at the observed drop-lock frequency offset is above the SDA/SSA SNR threshold for each of the nine drop-lock cases. While the actual mechanism causing the telemetry system (SDA) to drop lock is not yet understood, it is believed to be similar in nature to the "jump phenomenon" (Ref. 2) as observed in some phase lock loop receiver systems. That is, when two signals are simultaneously present in a PLL receiver, and if the two signals are within the PLL receiver's frequency capture range, the receiver's tracking loop tends to track the stronger signal. (This occurs even when the PLL receiver is initially locked to the weaker signal.) Regardless of the specific cause, for this analysis, let us assume that the telemetry system (SDA) will drop lock when the following condition is satisfied: (in algebraic format)

$$\left(R\,\frac{P_{ID}}{P_D}\right)^U \geqslant \left(\frac{\Delta f_{nsc}}{BR}\right)$$

Expressing the above relationship in decibel format:

$$U\left[P_{ID} - P_D + 10\log(R)\right] \geqslant \left[10\log\left(\frac{\Delta f_{nsc}}{BR}\right)\right]$$

where

$$P_{ID} = P_{RFI} - (.94)(20\log n)$$

P_D = data power in dBm

$$\Delta f_{nsc} \geqslant BR$$

By fitting the eight drop-lock data points to the above relationship, it is found that the drop-lock condition is:

$$0.65\,(P_{ID} - P_D - 3) \geqslant \left[10\log\left(\frac{\Delta f_{nsc}}{BR}\right)\right]$$

Also, for $\Delta f_{nsc} < BR$, it is expected that the drop-lock condition is

$$(P_{ID} - P_D - 3) \geqslant 0$$

Thus, the telemetry drop-lock model becomes:

For $\Delta f_{nsc} \geqslant BR$,

$$0.65\,(P_{ID} - P_D - 3) \geqslant \left[10\log\left(\frac{\Delta f_{nsc}}{BR}\right)\right]$$

For $\Delta f_{nsc} < BR$,

$$(P_{ID} - P_D - 3) \geqslant 0 \qquad (9)$$

where

$$P_{ID} = P_{RFI} - (.94)(20 \log n)$$

Using Eq. (9), a telemetry drop-lock profile is plotted against the test data on Fig. 25.

VIII. Summary of Analysis Results

When an interfering signal is present in addition to white Gaussian system noise, the telemetry signal is degraded. For CW signal interference, the following was observed:

(1) There is no observable degradation on telemetry data when the interfering signal is placed on any even subcarrier harmonic.

(2) There is observable degradation on telemetry data when the interfering signal is placed on an odd subcarrier harmonic.

Treating the CW interfering signal as a noise source to the telemetry system, the bit SNR degradation is modeled:

$$\Delta SNR_O = SNR_I - (L_S - L_{SR})$$

$$\Delta SNR_I = 10 \log \left(\frac{T_S + T_R}{T_S} \right)$$

where:

$$T_R \Big|_{BR=2K} = \left[\left(10^{821 e^{.0421 P_I}} \right)^2 + (40)^2 \right]^{1/2} - 39.5$$

$$P_I = P_{RFI} - (0.94)(20 \log n)$$

$$+ (0.90) \left(10 \log \left\{ \frac{\sin \left[\Delta f_{nsc} \left(\frac{\pi}{BR} \right) \right]}{\Delta f_{nsc} \left(\frac{\pi}{BR} \right)} \right\}^2 \right)$$

$$n = 1, 3, 5, \text{etc.}$$

The BER is found to be:

$$BER_R = 1/2 \; erfc \sqrt{\lambda}$$

where

$$\lambda = SNR_O - (0.79)(\Delta SNR_O)$$

In some severe cases, a CW interfering signal will cause the telemetry (SDA) system to drop lock. The drop-lock condition is

For

$$\Delta f_{nsc} \geqslant BR,$$

$$0.65 (P_{ID} - P_D - 3) \geqslant \left[10 \log \left(\frac{\Delta f_{nsc}}{BR} \right) \right]$$

For

$$\Delta f_{nsc} < BR,$$

$$(P_{ID} - P_D - 3) \geqslant 0$$

where

$$P_{ID} = P_{RFI} - (0.94)(20 \log n)$$

IX. Conclusions

The test configuration and procedures used for this investigation provided a very effective and efficient way of RFI generation, control, and data collection. Forty-two CW signal interference cases were tested. Empirical telemetry bit SNR and BER degradation and drop-lock models were developed based on the test data and certain physical characteristics of the telemetry system. Although the test used a 2000-bps data rate configuration, and the telemetry bit SNR degradation model derived was for 2000 bps data rate only, the results showed some very interesting and vital characteristics of the CW interfering signal's effects on the telemetry signal (system).

Additional tests and analysis are needed to better understand RFI effects on telemetry signal. Some major tasks will include further development of models to characterize:

(1) CW interfering signal's effect on telemetry signal as a function of various telemetry parameters (e.g., data rate).

(2) Continuous spectrum interference effects on telemetry signal.

References

1. Edelson, R. E., *Telecommunications System Design Techniques Handbook,* Technical Memorandum 33-571, Jet Propulsion Laboratory, Pasadena, California, July 15, 1972.

2. Kliger, I. E., and Olenberger, C. F., "PLL Jump Phenomenon in the Presence of Two Signals," *IEEE Trans. Aerospace Electron. Systems,* Vol. AES-12, Jan. 1976.

Table 1. Desired downlink signal configuration

Carrier frequency (f_c)	2293.148160 MHz
Carrier power (P_c)	See Tables 2 - 5
High rate data	
Subcarrier frequency (f_{sc1})	240 kHz
Data format	Uncoded
Bit rate (BR)	2000 bps
Modulation index	66.54 deg
Data power (P_D)	See Tables 2 - 5
Low rate data	
Subcarrier frequency	24 kHz
Data format	Uncoded
Bit rate	33-1/3 bps
Modulation index	19.25 deg
Data power	(P_c - 9.1) dBm

Table 2. Test cases of interfering signal coincident with subcarrier

Test number	P_C, dBm	P_D, dBm	SNT, °K	P_{RFI}, dBm	f_{RFI}
1A	-145.7	-138.5	28	-138.2	$f_c - f_{sc1}$
1B	-145.7	-138.5	28	-141.0	
1C	-145.7	-138.5	28	-144.0	
1D	-145.7	-138.5	28	-147.0	
1E	-145.7	-138.5	28	-150.0	
1F	-147.7	-138.5	28	-154.0	
1G	-145.7	-138.5	28	-164.0	
1H	-148.7	-141.5	28	-144.0	$f_c - f_{sc1}$
1I	-148.7	-141.5	28	-149.0	
1J	-148.7	-141.5	28	-153.7	
1K	-148.7	-141.5	28	-159.6	
1L	-148.7	-141.5	28	-168.0	
1M	-146.6	-139.4	26	-137.4	$f_c + f_{sc1}$
1N	-146.6	-139.4	26	-141.2	
1O	-146.6	-139.4	26	-146.2	
1P	-146.6	-139.4	26	-150.0	
1Q	-146.6	-139.4	26	-154.5	
1R	-146.6	-139.4	26	-158.0	
1S	-146.6	-139.4	26	-162.4	
1T	-146.6	-139.4	26	-164.6	
1U	-149.6	-142.4	26	-144.3	$f_c + f_{sc1}$
1V	-149.6	-142.4	26	-147.0	
1W	-149.6	-142.4	26	-150.0	
1X	-149.6	-142.4	26	-155.0	
1Y	-149.6	-142.4	26	-160.2	
1Z	-149.6	-142.4	26	-164.5	

Table 3. Test cases of subcarrier sweep

Test Number	$P_{C'}$ dBm	$P_{D'}$ dBm	SNT, °K	$P_{RFI'}$ dBm	Sweep rate, Hz/sec
2A	−147.0	−139.8	35.9	−120.0	30
2B	−147.0	−139.8	35.9	−123.0	↓
2C	−147.0	−139.8	35.9	−125.0	
2D	−147.0	−139.8	35.9	−130.0	
2E	−147.0	−139.8	35.9	−135.0	
2F	−147.0	−139.8	35.9	−140.0	

Table 4. Test cases of subcarrier 3rd harmonic sweep

Test Number	$P_{C'}$ dBm	$P_{D'}$ dBm	SNT, °K	$P_{RFI'}$ dBm	Sweep rate, Hz/sec
3A	−147.0	−139.8	35.9	−120.0	30
3B	−147.0	−139.8	35.9	−125.0	↓
3C	−147.0	−139.8	35.9	−130.0	
3D	−147.0	−139.8	35.9	−135.0	
3E	−147.0	−139.8	35.9	−140.0	

Table 5. Test cases of subcarrier 5th harmonic sweep

Test Number	$P_{C'}$ dBm	$P_{D'}$ dBm	SNT, °K	$P_{RFI'}$ dBm	Sweep rate, Hz/sec
4A	−147.0	−139.8	35.9	−120.0	30
4B	−147.0	−139.8	35.9	−125.0	↓
4C	−147.0	−139.8	35.9	−130.0	
4D	−147.0	−139.8	35.9	−135.0	
4E	−147.0	−139.8	35.9	−140.0	

Table 6. BER vs λ for an uncoded channel

λ		BER	λ		BER
Ratio	dB		Ratio	dB	
0.080	−10.969	.34458	3.125	4.948	.00621
0.125	−9.031	.30854	3.380	5.289	.00466
0.180	−7.447	.27425	3.645	5.617	.00347
0.245	−6.108	.24196	3.920	5.933	.00256
0.320	−4.948	.21185	4.205	6.238	.00187
0.405	−3.925	.18406	4.500	6.532	.00135
0.500	−3.010	.15865	4.805	6.817	.0009689
0.605	−2.182	.13566	5.120	7.093	.0006882
0.720	−1.427	.11507	5.445	7.360	.0004843
0.845	−0.731	.09680	5.780	7.619	.0003377
0.980	−0.088	.08056	6.125	7.871	.0002333
1.125	9.512	.06681	6.480	8.116	.0001597
1.280	1.072	.05480	6.845	8.354	.0001082
1.445	1.599	.04457	7.220	8.585	.0000727
1.620	2.095	.03593	7.605	8.811	.0000484
1.805	2.565	.02872	8.405	9.245	.0000209
2.000	3.010	.02275	9.245	9.659	.0000087
2.205	3.434	.01787	10.125	10.045	.0000036
2.420	3.838	.01391	11.045	10.432	.0000015
2.645	4.224	.01073	12.005	10.792	.0000006
2.880	4.594	.00820			

[a]Source: Ref. 1, p. 143.

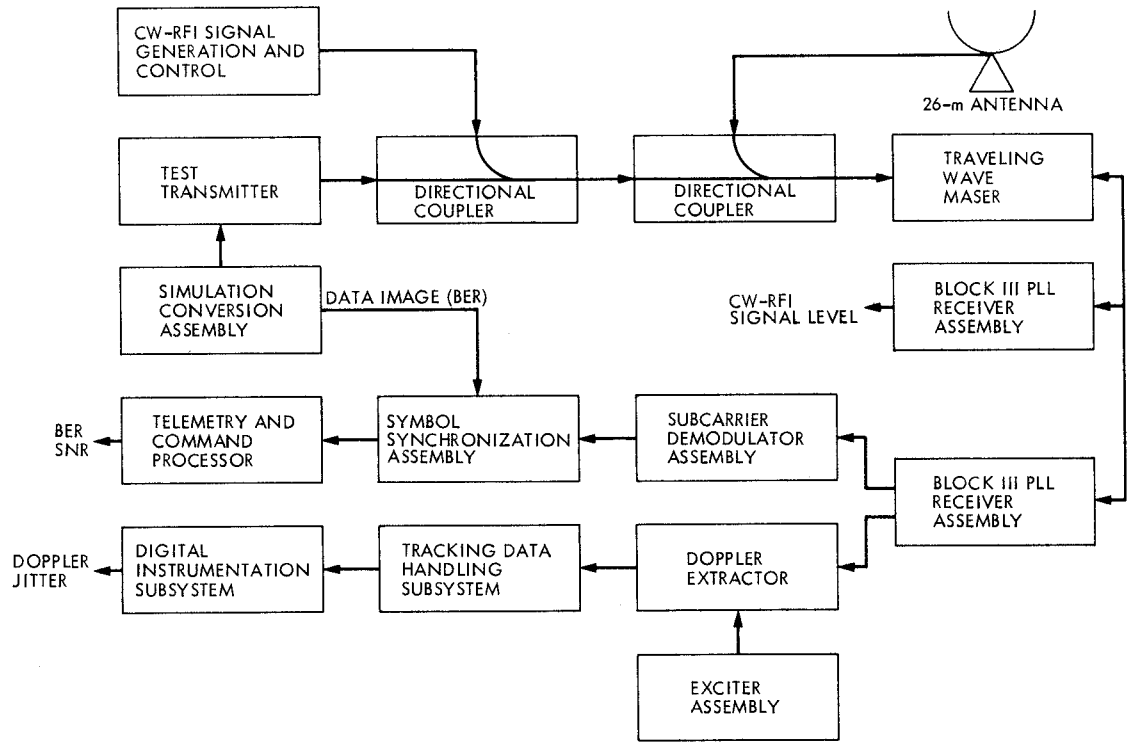

Fig. 1. Test configuration

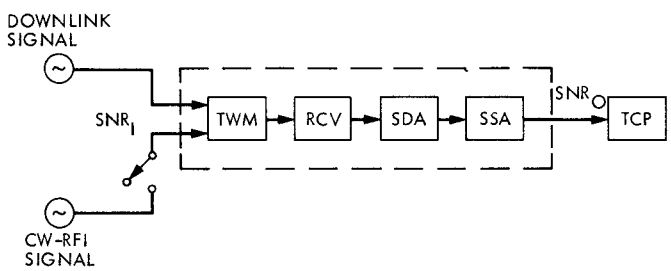

Fig. 2. Simplified carrier tracking and telemetry processing system

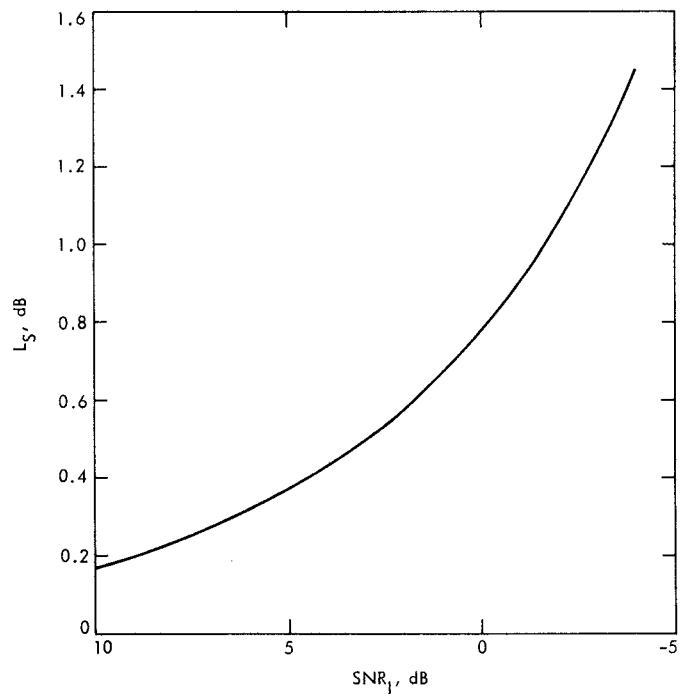

Fig. 3. Theoretical system loss curve (for test configuration)

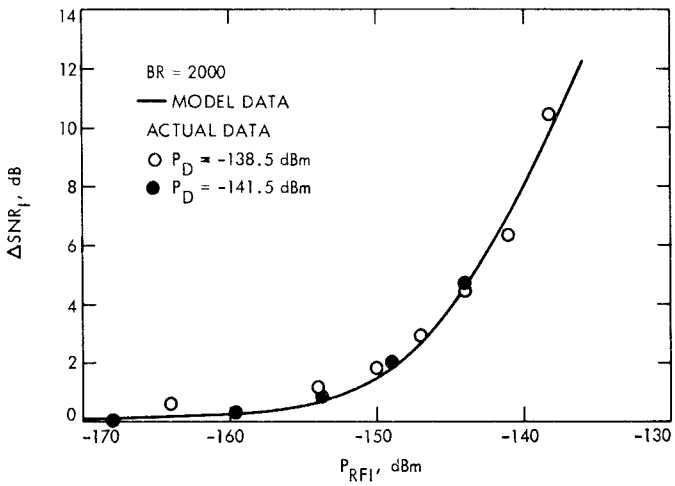

Fig. 4. Received telemetry bit SNR degradation (ΔSNR_I) vs CW interfering signal level (P_{RFI}) for $\Delta f_{1sc} = 0$ at SNT = 28°K

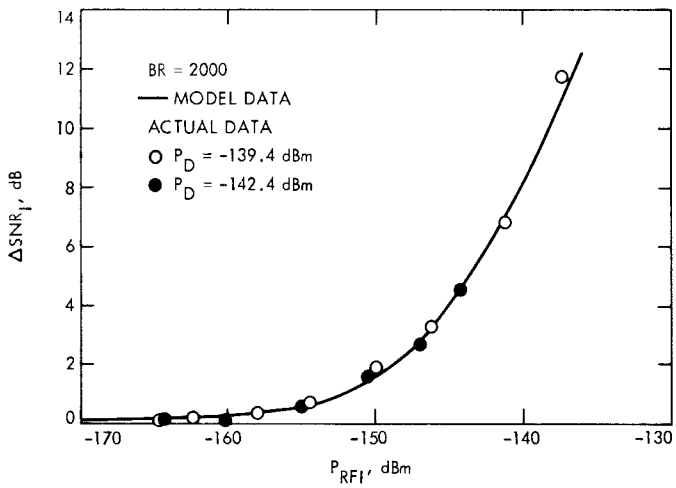

Fig. 5. Received telemetry bit SNR degradation (ΔSNR_I) vs CW interfering signal level (P_{RFI}) for $\Delta f_{1sc} = 0$ at SNT = 26°K

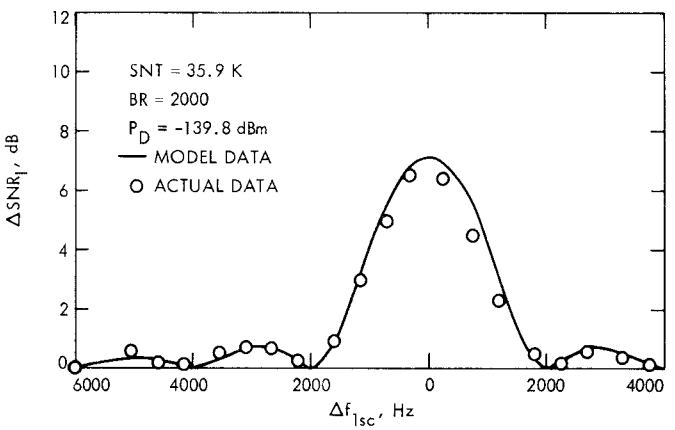

Fig. 6. Received telemetry bit SNR degradation (ΔSNR_I) vs frequency offset between subcarrier and CW interfering signal (Δf_{1sc}) for $P_{RFI} = -140$ dBm

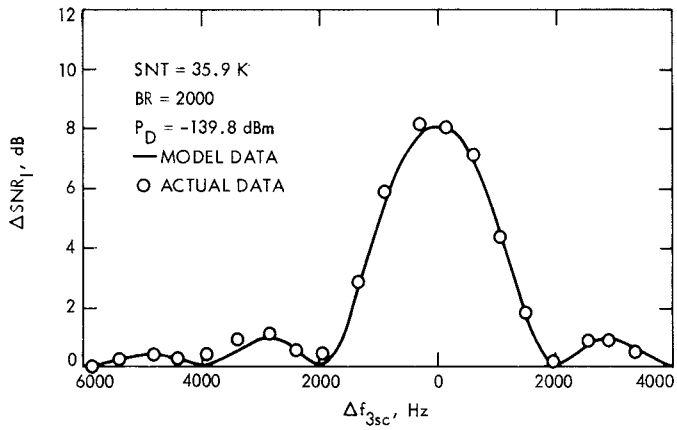

Fig. 7. Received telemetry bit SNR degradation (ΔSNR_I) vs frequency offset between subcarrier third harmonic and CW interfering signal (Δf_{3sc}) for $P_{RFI} = -130$ dBm

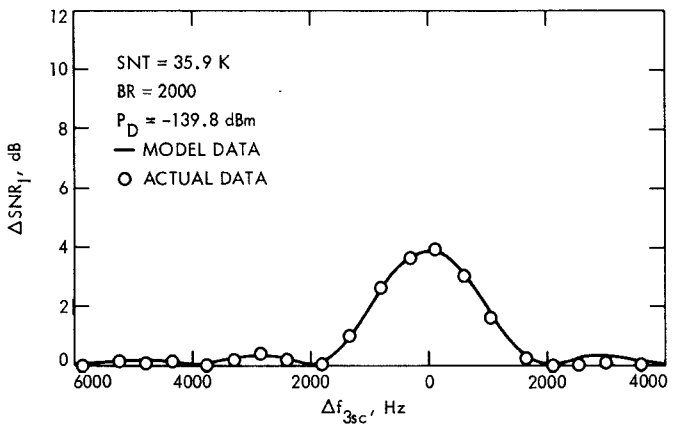

Fig. 8. Received telemetry bit SNR degradation (ΔSNR_I) vs frequency offset between subcarrier third harmonic and CW interfering signal (Δf_{3sc}) for P_{RFI} = −135 dBm

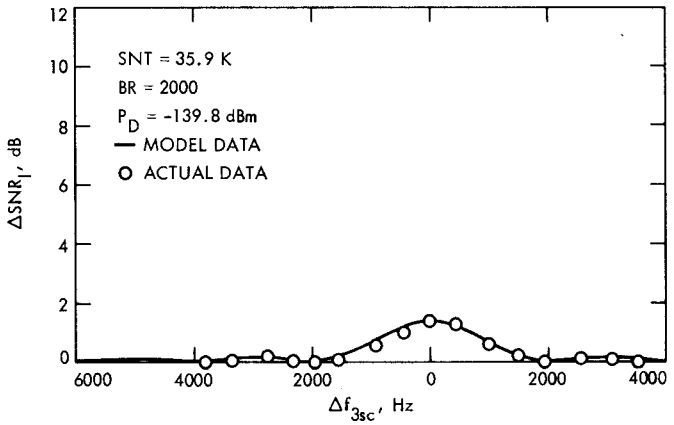

Fig. 9. Received telemetry bit SNR degradation (ΔSNR_I) vs frequency offset between subcarrier third harmonic and CW interfering signal (Δf_{3sc}) for P_{RFI} = −140 dBm

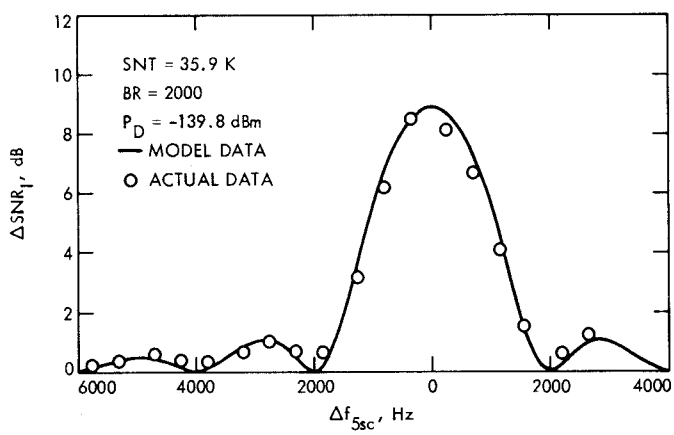

Fig. 10. Received telemetry bit SNR degradation (ΔSNR_I) vs frequency offset between subcarrier fifth harmonic and CW interfering signal (Δf_{5sc}) for P_{RFI} = −125 dBm

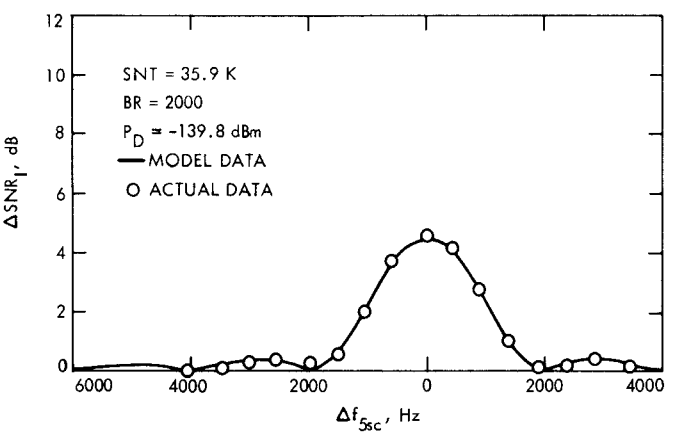

Fig. 11. Received telemetry bit SNR degradation (ΔSNR_I) vs frequency offset between subcarrier fifth harmonic and CW interfering signal (Δf_{5sc}) for P_{RFI} = −130 dBm

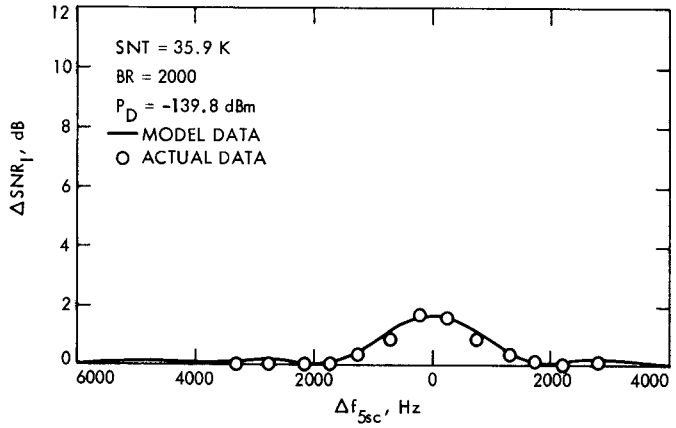

Fig. 12. Received telemetry bit SNR degradation (ΔSNR_I) vs frequency offset between subcarrier fifth harmonic and CW interfering signal (Δf_{5sc}) for P_{RFI} = −135 dBm

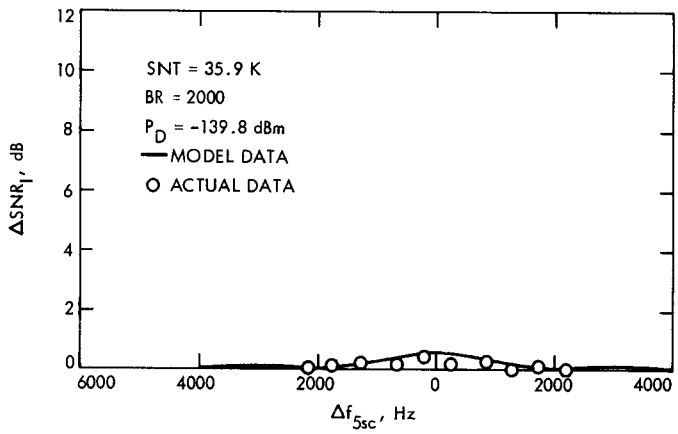

Fig. 13. Received telemetry bit SNR degradation (ΔSNR_I) vs frequency offset between subcarrier fifth harmonic and CW interfering signal (Δf_{5sc}) for P_{RFI} = −140 dBm

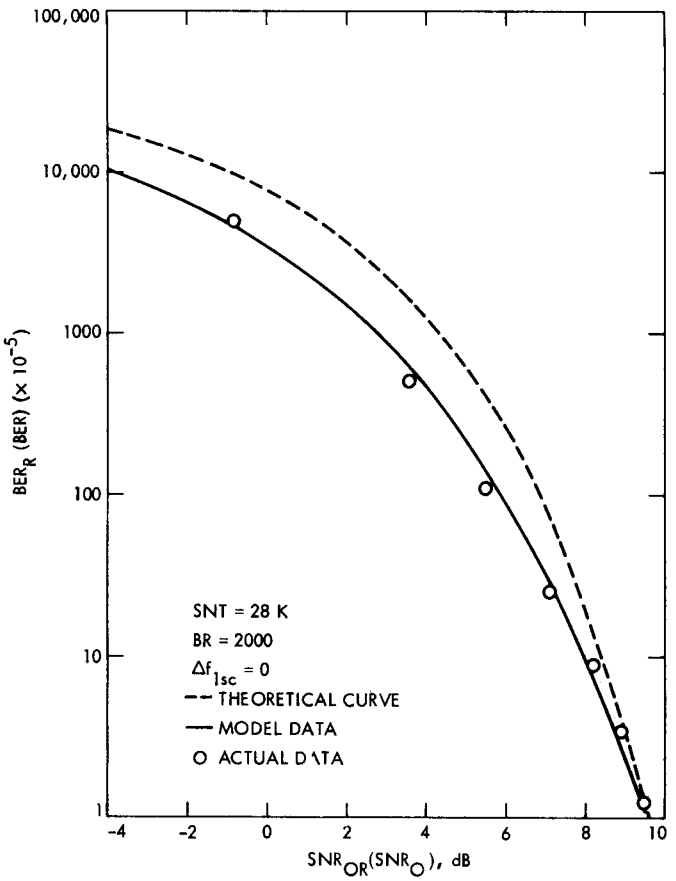

Fig. 14. Theoretical BER curve (*BER* vs *SNR*) and BER in the presence of CW interference (BER_R vs SNR_{OR}) for the case of P_D = −138.5 dBm

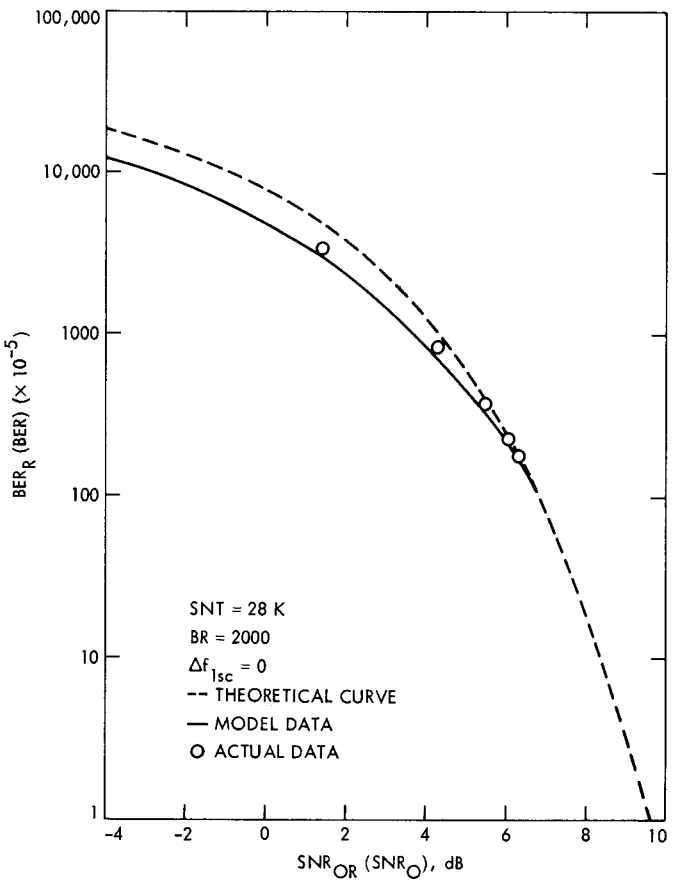

Fig. 15. Theoretical BER curve (*BER* vs SNR_O) and BER in the presence of CW interference (BER_R vs SNR_{OR}) for the case of P_D = −141.5 dBm

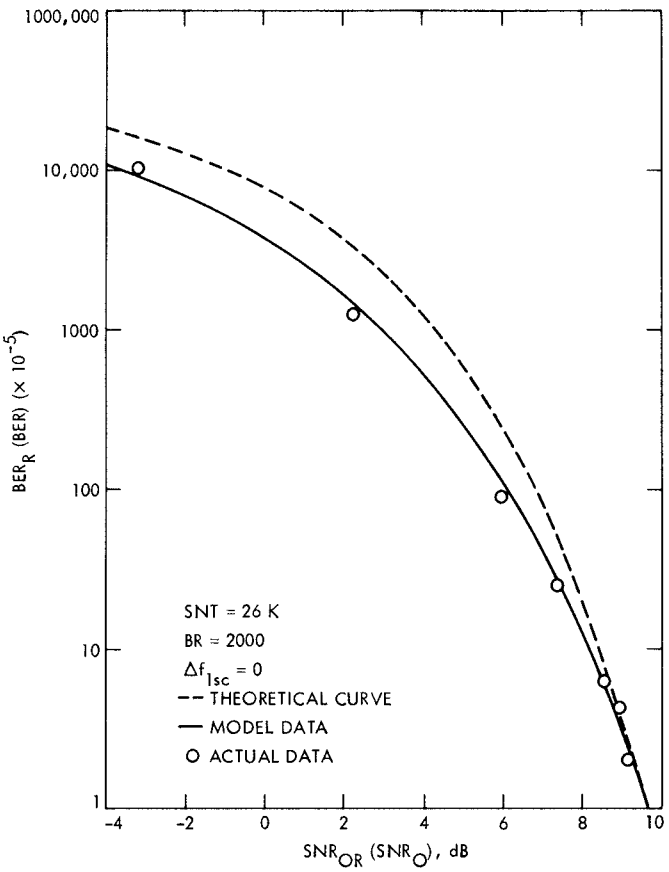

Fig. 16. Theoretical BER curve (*BER* vs SNR_O) and BER in the presence of CW interference (BER_R vs SNR_{OR}) for the case of P_D = −139.4 dBm

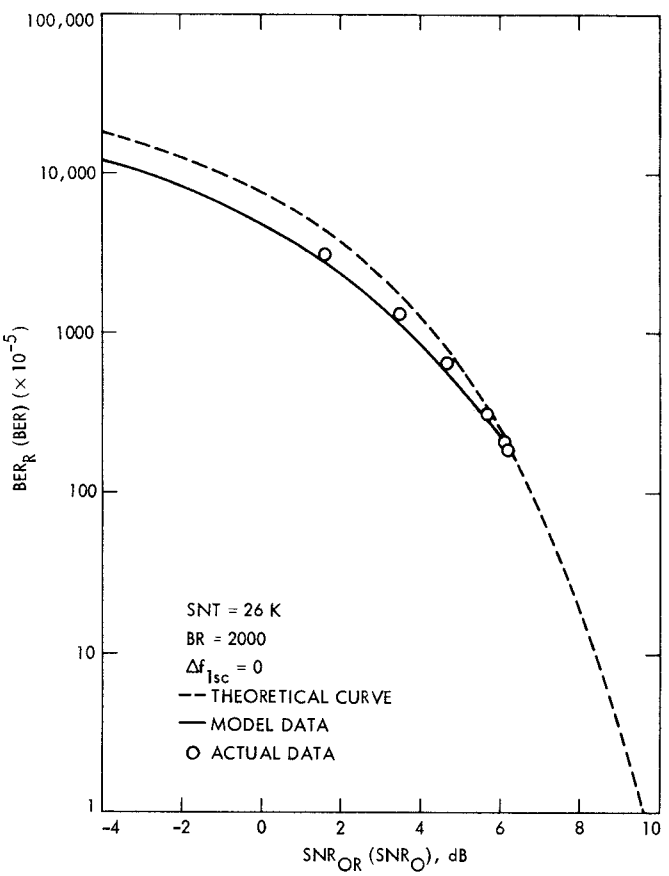

Fig. 17. Theoretical BER curve (*BER* vs SNR_O) and BER in the presence of CW interference (BER_R vs SNR_{QR}) for the case of P_D = −142.4 dBm

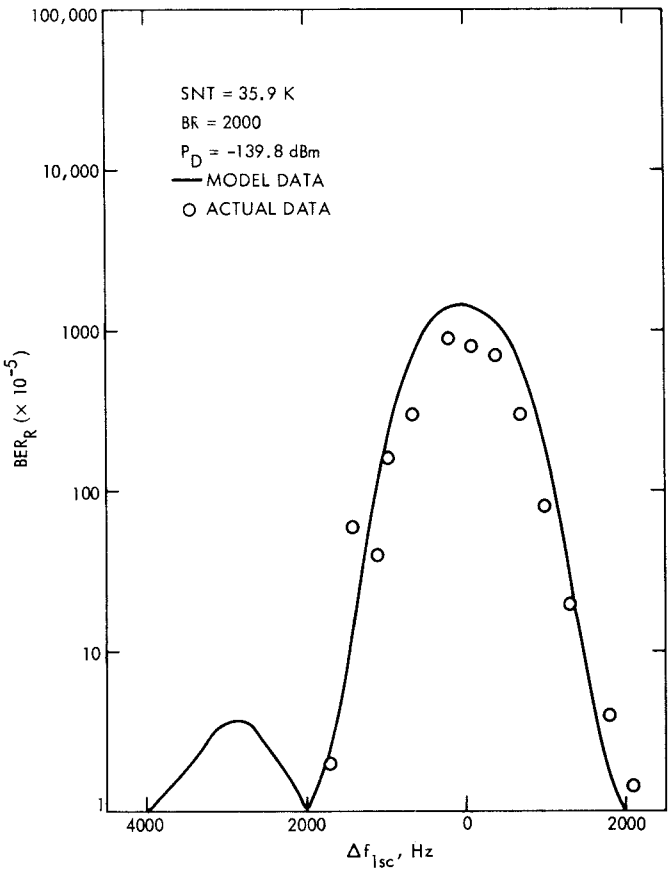

Fig. 18. Telemetry BER degradation (BER_R) vs frequency offset between subcarrier and CW interfering signal (Δf_{1sc}) for P_{RFI} = −140 dBm

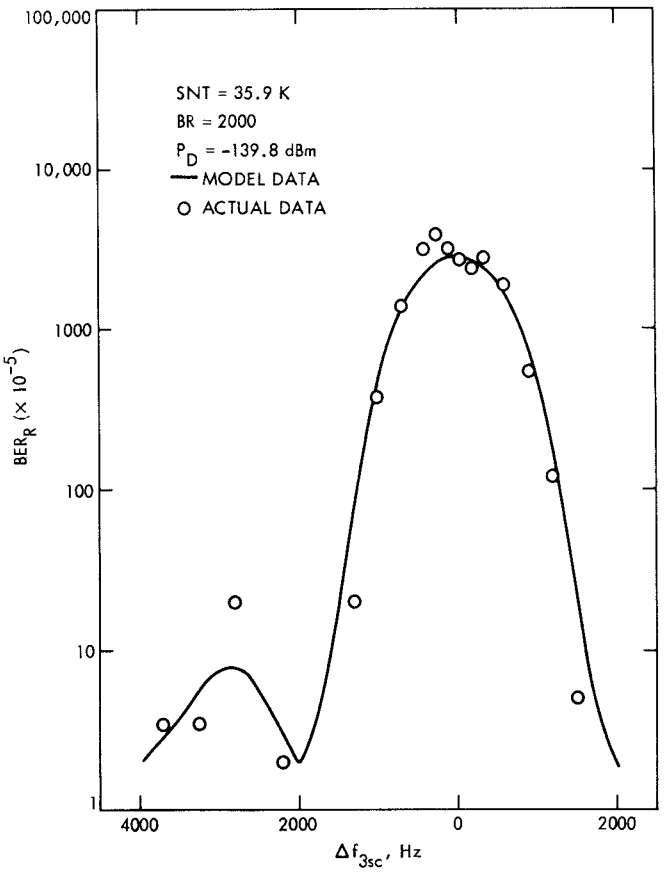

Fig. 19. Telemetry BER degradation (BER_R) vs frequency offset between subcarrier third harmonic and CW interfering signal (Δf_{3sc}) for P_{RFI} = −130 dBm

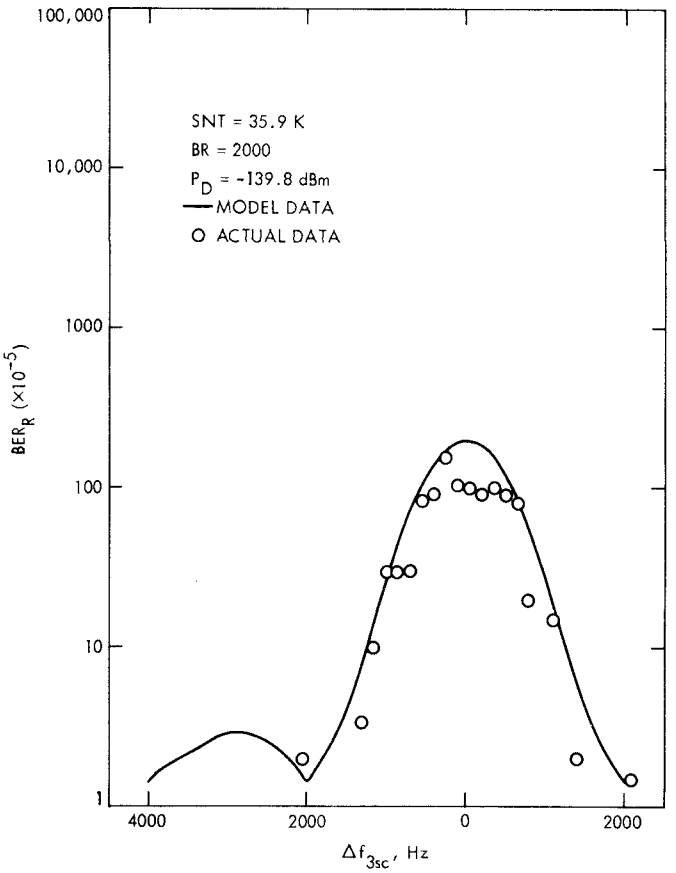

Fig. 20. Telemetry BER degradation (BER_R) vs frequency offset between subcarrier third harmonic and CW interfering signal (Δf_{3sc}) for P_{RFI} = −135 dBm

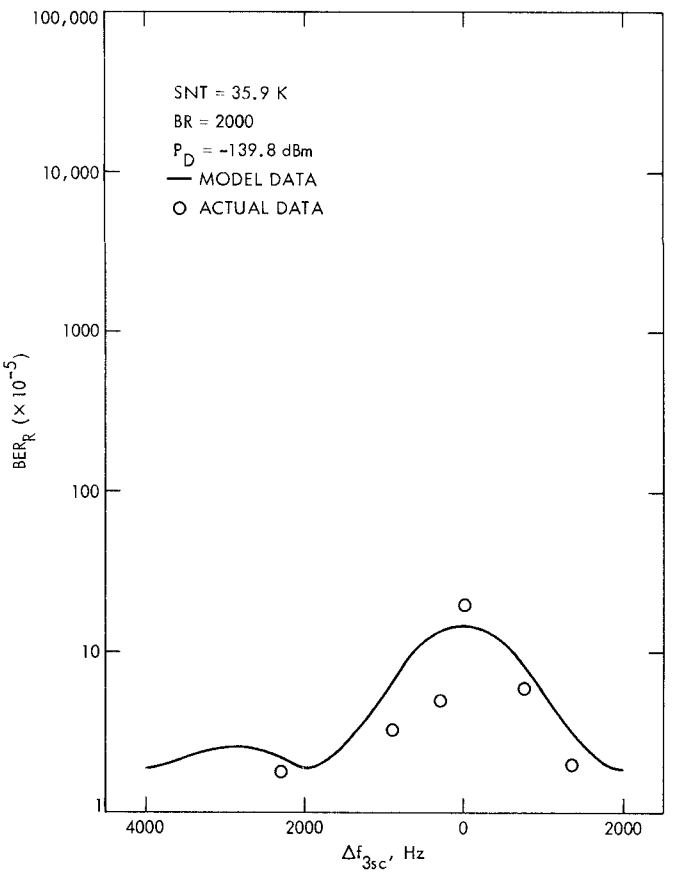

Fig. 21. Telemetry BER degradation (BER_R) vs frequency offset between subcarrier third harmonic and CW interfering signal (Δf_{3sc}) for P_{RFI} = −140 dBm

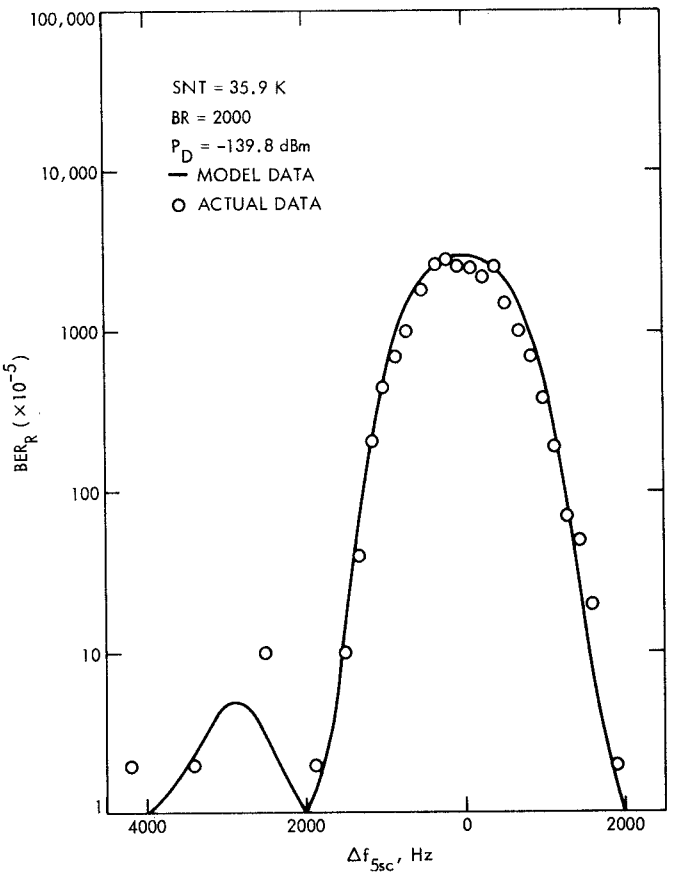

Fig. 22. Telemetry BER degradation (BER_R) vs frequency offset between subcarrier fifth harmonic and CW interfering signal (Δf_{5sc}) for P_{RFI} = −125 dBm

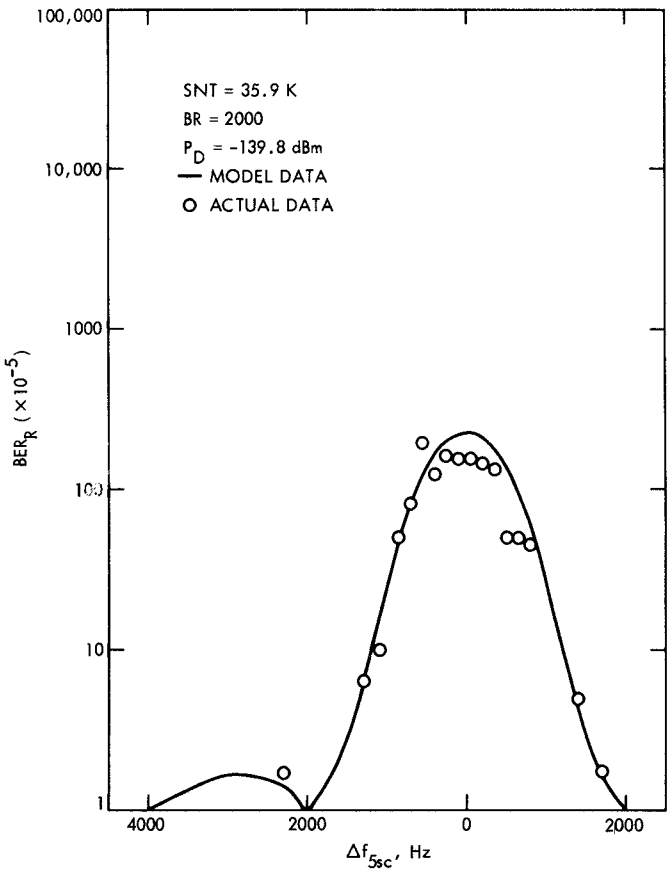

Fig. 23. Telemetry BER degradation (BER_R) vs frequency offset between subcarrier fifth harmonic and CW interfering signal (Δf_{5sc}) for P_{RFI} = −130 dBm

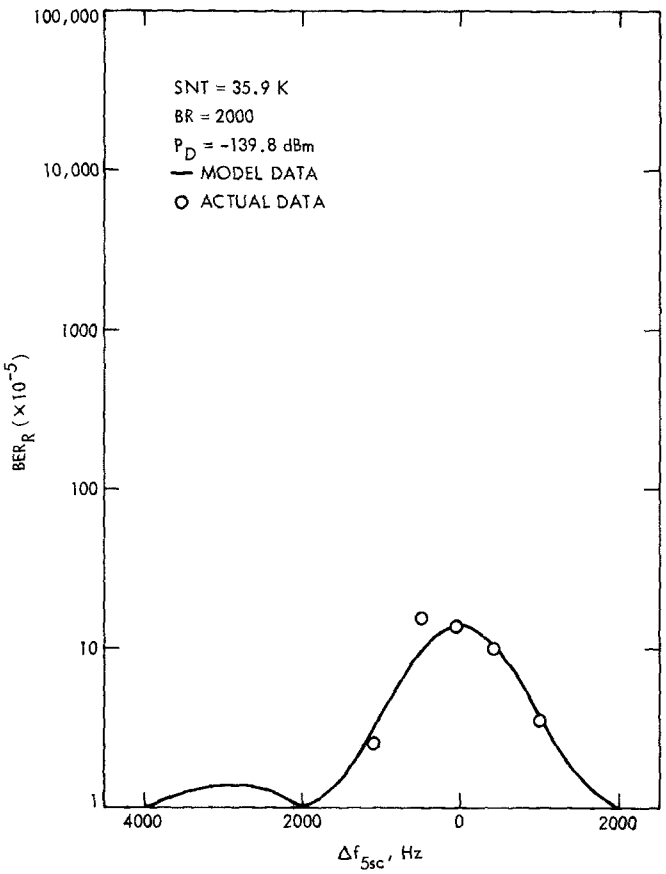

Fig. 24. Telemetry BER degradation (BER_R) vs frequency offset between subcarrier fifth harmonic and CW interfering signal (Δf_{5sc}) for P_{RFI} = −135 dBm

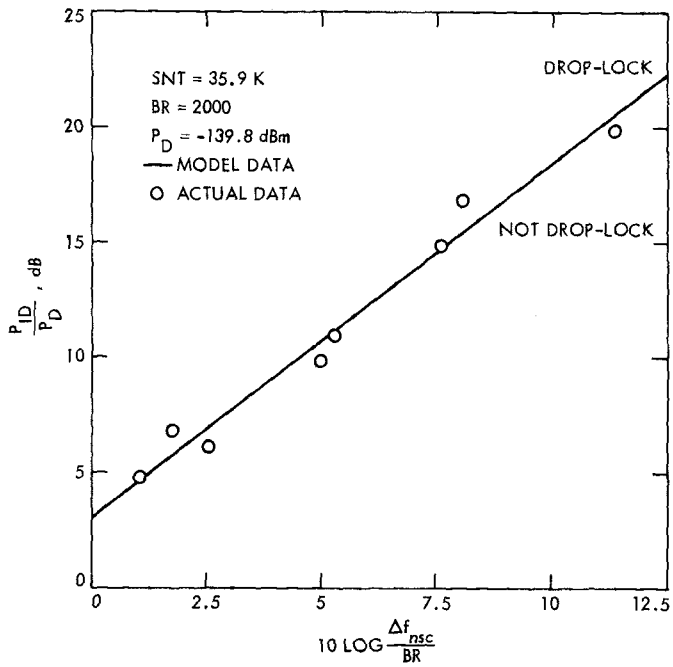

Fig. 25. Telemetry drop-lock profile